Atmospheric Pollution Research 9 (2018) 309–321

HOSTED BY

Contents lists available at ScienceDirect

Atmospheric Pollution Research

journal homepage: http://www.journals.elsevier.com/locate/apr

Characteristics of mass concentration, chemical composition, source apportionment of $PM_{2.5}$ and PM_{10} and health risk assessment in the emerging megacity in China

Nan Jiang, Shasha Yin*, Yue Guo, Jingyi Li, Panru Kang, Ruiqin Zhang**, Xiaoyan Tang

Research Institute of Environmental Science, College of Chemistry and Molecular Engineering, Zhengzhou University, Zhengzhou, 450001, China

ARTICLE INFO

Article history:
Received 4 June 2017
Received in revised form
12 July 2017
Accepted 12 July 2017
Available online 6 November 2017

Keywords:
$PM_{2.5}$
PM_{10}
Chemical characteristics
Source apportionment
Carcinogenic risks

ABSTRACT

In this study, 228 daily Particulate matter (PM) filters (57 Quartz and 57 Teflon samples for both $PM_{2.5}$ and PM_{10}, respectively) were collected from an urban site in Zhengzhou in typical months from 2014 autumn to 2015 summer representing the four seasons. PM concentrations, water-soluble inorganic ions, organic carbon, elemental carbon, and elements were determined, and positive matrix factorization was used for source apportionments. Health risks of toxic elements in $PM_{2.5}$ and PM_{10} were also evaluated. The annual mean values of $PM_{2.5}$ and PM_{10} were higher than the standards in China, and the highest seasonal concentrations of $PM_{2.5}$ and PM_{10} were in winter. Secondary inorganic aerosols (SIAs) were the major component, with the ratio of SIAs/PM highest in summer. The seasonal concentrations of SO_4^{2-} were high in winter and summer. Crustal elements mainly existed in $PM_{2.5-10}$; however, elements from anthropogenic sources (i.e., Zn, Pb, Cu, As, Cd, and Mo) were more abundant in fine particles than in the coarse fraction. The main pollution sources were dust, SIAs, coal combustion, vehicle and road dust, and industry, accounting for 10%, 26%, 25%, 20% and 15% in $PM_{2.5}$ and 32%, 14%, 24%, 18% and 8% in PM_{10}, respectively. Dust source has the highest contribution in PM_{10}; however, SIAs source has the highest content in fine particles. The carcinogenic risks of As to children through the daily intake pathway in $PM_{2.5}$ and PM_{10} exceeded the acceptable level. Noncarcinogenic risks of As and Cd in $PM_{2.5}$ and PM_{10} to children via the daily intake pathway were significant. Moreover, the sum of noncarcinogenic risks in PM_{10} via inhalation exposure for local residents and that via dermal absorption for children were significant. The details of the pollution characteristics and the results of source apportionments and health risks assessment of $PM_{2.5}$ and PM_{10} in this study can play an important role for the government to formulate reasonable and effective policy to mitigate the atmospheric pollution of PM. To our knowledge, this systematic study is the first to investigate the chemical characterizations, source apportionments, and health effects of $PM_{2.5}$ and PM_{10} in Zhengzhou.

1. Introduction

In recent years, with the rapid industrialization and urbanization in China, atmospheric particulate matter (PM) has been one of the most important air contaminants. PM, particularly $PM_{2.5}$ (aerodynamic diameter $\leq$ 2.5 μm) and PM_{10} (aerodynamic diameter $\leq$ 10 μm), is closely associated with haze, with a serious impact on global and regional climate changes, reduced visibility, and human health effects (Kang et al., 2004; Bytnerowicz et al., 2007; Moosmüller et al., 2009; Tan et al., 2009; Cheng et al., 2011).

The main chemical components of PM, including water-soluble inorganic ions (WSIIs), organic carbon (OC), elemental carbon (EC), and elements, were investigated in several studies in China (Fu et al., 2008; Gao et al., 2015; Lai et al., 2016). WSIIs, dominated by secondary inorganic aerosols (SIAs) including NH_4^+, NO_3^-, and SO_4^{2-}, and the ratio of SIAs/$PM_{2.5}$ increased during haze episodes (Wang et al., 2012). OC, composed of thousands of organic compounds,

* Corresponding author.
** Corresponding author.
E-mail addresses: shashayin@zzu.edu.cn (S. Yin), rqzhang@zzu.edu.cn (R. Zhang).

Peer review under responsibility of Turkish National Committee for Air Pollution Research and Control.

https://doi.org/10.1016/j.apr.2017.07.005
1309-1042/

contains many toxic substances and has attracted considerable attention (Wang et al., 2015). Heavy metals, such as Pb, Cd, Cu, Zn, and Cr, represent a consistent part of the trace elements in PM (Geng et al., 2013; Querol et al., 2007).

The chemical composition and particle size distribution characteristics of PM play an important role in the comprehension of its sources, formation and transport process (Yin and Harrison, 2008; Putaud et al., 2010). The result of source apportionment is the essential to formulate policies for the government to control PM pollution. In fact, sources of $PM_{2.5}$ and PM_{10} are complex, including a variety of anthropogenic and natural sources (Querol et al., 2007). In addition, PM is directly released from the sources or formed as secondary pollutants from the primary emissions through photochemical reactions. The most widely used methods in source apportionment are receptor models. Positive matrix factorization (PMF) is one of the most broadly used receptor models (Wang et al., 2013; Kassomenos et al., 2014; Cesari et al., 2016; Manousakas et al., 2016).

In recent years, in China, most studies have generally concentrated on the Yangtze River Delta, Pearl River Delta and Jing-Jin-Ji region with severe atmospheric environments (Ye et al., 2003; Chan and Yao, 2008; Fu et al., 2008). The key areas of atmospheric control identified by the Chinese government in the National Clean Air Action Plan, which was released by the State Council in September 2013, are also concentrated in this region. Only a few scholars have investigated $PM_{2.5}$ pollution in Zhengzhou, which was predicted by the Economist Intelligence Unit to become an emerging megacity around 2020, similar to the megalopolises (i.e., Beijing, Shanghai, and Guangzhou) (https://www.eiu.com/public/topical_report.aspx?campaignid=Megalopolis2012). By the end of 2015, Zhengzhou had a population of 9.57 million, with the annual Gross Domestic Product of USD 106.09 billion, which is a 10.1% increase from the previous year, and the number of motor vehicles was 2.39 million (Bureau of Statistics of Henan Province, 2016). With the extensive economic growth mode, PM pollution occurs frequently in Zhengzhou (http://public.zhengzhou.gov.cn/service140201/221015.jhtml), seriously affecting people's lives. However, several studies focused on the component concentration and source apportionment of $PM_{2.5}$ over a specific sampling period only (Wang et al., 2015; Yu et al., 2016; Jiang et al., 2017b), without comparing the different characteristic between $PM_{2.5}$ and PM_{10}, not to mention the health effects.

In this study, Zhengzhou is chosen as the study area to conduct sampling of typical seasonal $PM_{2.5}$ and PM_{10} for one year. The concentrations of $PM_{2.5}$ and PM_{10}, WSIIs, OC, EC and elements are analyzed and discussed in the current study. The PMF is used for $PM_{2.5}$ and PM_{10} source apportionments to analyze the differences of pollution sources between different particle sizes. This study also aimed at estimating the carcinogenic and noncarcinogenic health risks of toxic elements in PM to the exposed local residents. The details of the pollution characteristics and the results of source apportionments and health risks assessment of $PM_{2.5}$ and PM_{10} in this study can provide the government with reasonable and effective measures to mitigate the atmospheric pollution of PM.

2. Materials and methods

2.1. Sample collection

The atmospheric PM samples were collected in typical months from October 2014 to July 2015 representing the four seasons. The sampling site was located on the roof (14 m height) of the Collaborative Innovation Center of Henan Resources and Materials Industry in Zhengzhou University (113°31′ E; 34°48′ N) (Fig. 1.). Two high-volume sampling instruments (1.13 m^3/min; TE-6070D, Tisch, USA) and two low-volume sampling instruments (16.67 L/min; 2025i, Thermo, USA), with quartz microfiber filters (20.32 cm × 25.4 cm, for WSIIs, EC and OC analysis) and Teflon filters (47 mm in diameter, for mass concentration and element analysis), respectively, were used to collect $PM_{2.5}$ and PM_{10} samples. PM samples were collected once a day from 9:00 a.m. to 8:00 a.m. of the following day in four seasons.

Quartz filters were baked at 450 °C for 5 h in a muffle furnace before sampling to eliminate the possible presence of organics. All filters were placed in a super clean room (temperature of 25 ± 5 °C; relative humidity of 50± 5%) for 48 h and weighed by a high-precision electronic balance (Mettler Toledo XS205), with an accuracy of 10 μg before and after sampling. Each filter was weighed twice, with the difference between the two results not more than 0.3 mg for quartz filters and 0.03 mg for Teflon filters, to guarantee precision of the weighting results. All filters were stored in a freezer at −20 °C before analysis to prevent the loss of volatile components.

2.2. Chemical analysis

2.2.1. WSII analysis

The concentrations of anions (i.e., F^-, Cl^-, NO_3^- and SO_4^{2-}) and cations (i.e., Na^+, NH_4^+, K^+, Mg^{2+}, and Ca^{2+}) were measured by ion chromatography (ICS-90, ICS-900, Dionex, USA). Quartz filters were cut into pieces, each with an area of 10.9 cm^2. Two pieces of filters were soaked in 25 mL ultrapure water in a beaker and extracted for 30 min in an ultrasonic bath (<30 °C). The extracted solutions were filtered by 0.22 μm microporous membrane and analyzed.

2.2.2. OC and EC analysis

Two pieces of filters (each with an area of 2.0 cm^2) were removed from each quartz filter, and the thermal/optical transmittance method was chosen to determine OC and EC using a carbon analyzer (Sunset Laboratory, USA). OC and EC analysis consecutively proceeded through two temperature programmers. In the first stage, OC was volatilized from the filter in a pure helium atmosphere with the step by step increase in temperature to approximately 840 °C. In the second stage, the temperature was gradually increased to approximately 870 °C in an oxidizing atmosphere of 2% oxygen with 98% helium. Pyrolysis products were converted to CO_2 gas in a MnO_2 oxidizing oven. Then, CO_2 was directly measured by a self-contained nondispersive infrared detector system.

2.2.3. Element analysis

Teflon filters were used for element analysis. Each filter was cut into pieces in a crucible and baked in the muffle furnace at 300 °C maintained 40 min. Then, the temperature was gradually increased to 550 °C and remained constant for 1 h. After cooling, 0.2 g NaOH and a few drops of anhydrous ethanol were added into the crucible and baked again in the muffle furnace at 500 °C for 10 min. Then, 5 mL of pure water (90 °C) was added into the cooled crucible, and the extraction process was conducted at 100 °C on a hot plate. A total of 20 elements (e.g., Al, Fe, Mg, Zn, Pb, Co, As, and Cd) were analyzed via an inductively coupled plasma mass spectrometer (Agilent 7500cx, Santa Clara, CA, USA).

2.3. Quality assurance and quality control (QA/QC)

Field blank filters were analyzed to measure blank concentrations. The method detection limit (MDL) was calculated by three times the standard deviation of replicate instrumental measurements of spiked blanks (US EPA, 2016). Each sample was measured twice with the error acceptable within 5%.

For WSIIs, the field blank concentration values were 0.00, 0.01,

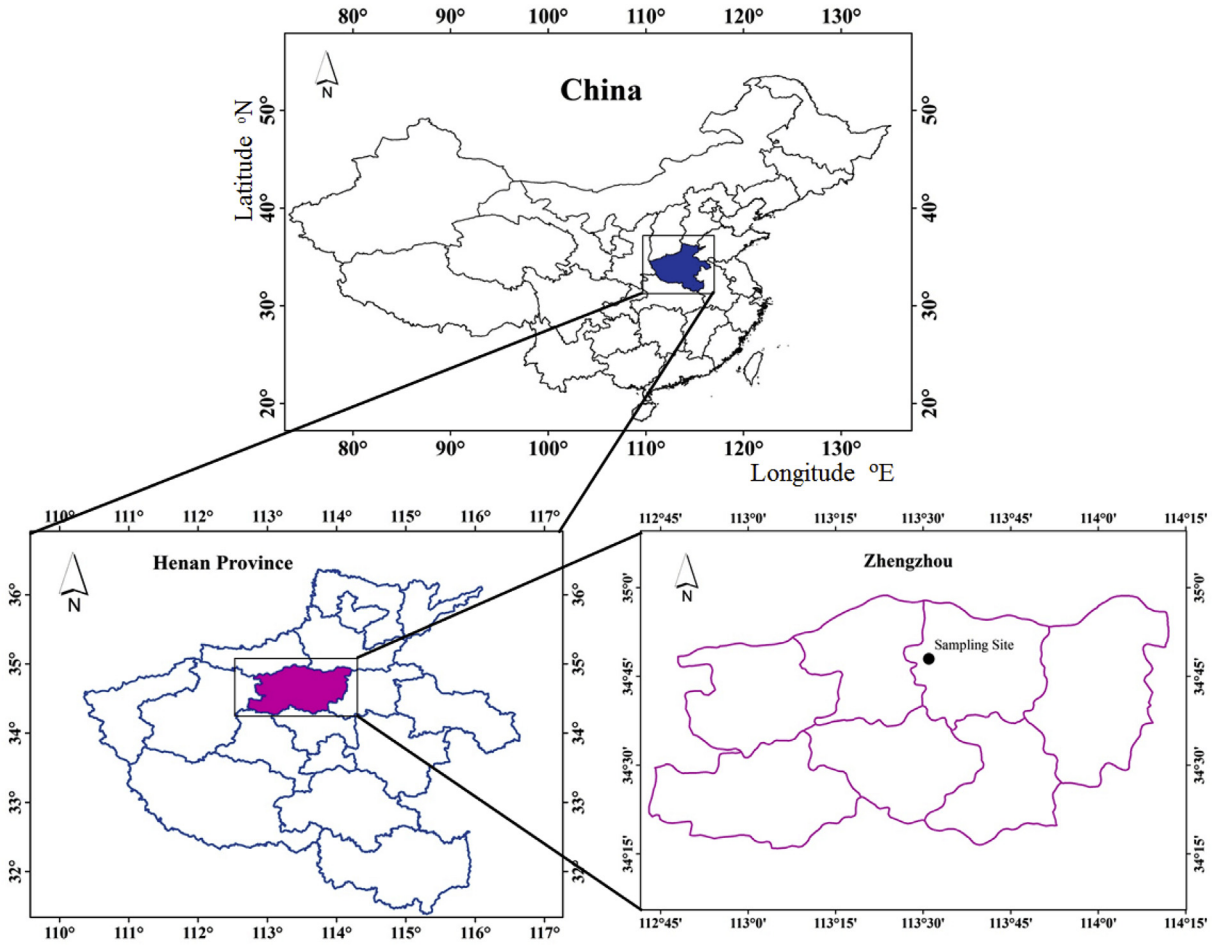

Fig. 1. Location of the sampling site in Zhengzhou, China.

0.00, 0.00, 0.02, 0.03, 0.00, 0.00 and 0.03 μg/m^3 for F^-, Cl^-, NO_3^-, SO_4^{2-}, Na^+, NH_4^+, K^+, Mg^{2+} and Ca^{2+}, respectively. The standard curve was used to analyze the samples quantitatively, and the R^2 values of the standard curve for all of the ions were higher than 0.999 (except for NH_4^+ at 0.99). The MDLs range from 0.06 μg/m^3 (NH_4^+) to 0.51 μg/m^3 (SO_4^{2-}). For the recovery test, the standard addition recovery of the nine ions ranged between 89% and 110%.

For OC and EC, the analyzer was calibrated via a sucrose standard solution before the experiment. A blank sample was measured every eight samples. The MDL was 0.2 μg/cm^2 for both OC and EC.

For elements, the standard recovery efficiencies were determined, with values ranging from 80% to 120%. The MDLs were calculated, and the values ranged from 0.001 μg/L (Ag) to 1.547 μg/L (Sb). The R^2 values of the standard curve of the elements were higher than 0.999.

For the expanded uncertainty, calculated by multiplying the uncertainty by a coverage factor (typically in the range 2–3) according to the National Institute of Standards and Technology (http://physics.nist.gov/cuu/Uncertainty/coverage.html), the value of each analytical method was 22%, 14% and 41% for WSIIs, OC and EC, and elements, respectively.

2.4. PMF modeling

PMF based on the weighted least square fit approach is an important and convenient factor analysis model (Paatero and Tapper, 1994). The model decomposes the sample data matrix into factor contribution matrix and factor profile matrix. More details are described by Shen et al. (2016) and Wang et al. (2017). In this study, PMF 5.0 was applied to the daily $PM_{2.5}$ and PM_{10} data at the sampling site, aiming at the identification and quantification of the major aerosol sources.

The sample species concentration and sample species uncertainty are the input data files for PMF. According to the PMF user guide and the previous studies (US EPA, 2014; Brown et al., 2015; Cesari et al., 2016), for data-pretreatment of the specie concentrations, the species median were used instead of the missing data, and the concentrations of 0.5 * MDL were used instead of the values below MDL. For the uncertainties, in the previous studies (Tauler et al., 2009; Jang et al., 2013), if the specie concentration was above the MDL, the uncertainty was considered to be 0.1 * concentration + MDL/3; if the specie concentration below MDL, the uncertainty was considered to be 0.2 * concentration + MDL/3; however, for the missing data, replaced with the species-specific median, all associated uncertainty value was a high uncertainty of four times the species-specific median (US EPA, 2014). For data outlier, the certain samples were excluded, and the species, without meeting the requirement of data analysis, were categorized as “Bad” and also excluded from the PMF analysis. More other details were described in the PMF 5.0 User Guide (US EPA, 2014).

2.5. Health risks assessment

2.5.1. Exposure assessment

Local residents are potential receptors of toxic elements in the

atmosphere, and the three main exposure pathways are inhalation, dermal absorption, and ingestion. The Human Health Evaluation Manual and Supplemental Guidance for Dermal and Inhalation Risk Assessment (Parts E and F) were provided by the US EPA (2011a). In this study, residents were divided into two groups, namely, children (<15 years) and adults, because of differences in behaviors and respiration (Hu et al., 2012), exposure concentration (EC_{inhale}, μg/m^3), dermal absorption dose (DAD_{dermal}, mg/(kg day)) and chemical daily intake (CDI_{ingest}, mg/(kg day)) of toxic elements in $PM_{2.5}$ and PM_{10} via the three pathways, which were calculated as follows:

$$EC_{inhale} = \frac{(C \times ET \times EF \times ED)}{AT_1} \quad (1)$$

$$DAD_{dermal} = \frac{C \times SA \times AF \times ABS}{BW} \times \frac{EF \times ED}{AT_2} \times CF \quad (2)$$

$$CDI_{ingest} = \frac{C \times IngR}{BW} \times \frac{EF \times ED}{AT_2} \times CF \quad (3)$$

where all parameters used in the three formulas were found in the reports published by the US EPA (2011a), unless otherwise indicated; C is the 95% upper confidence limit on the arithmetic mean concentrations of elements in $PM_{2.5}$ and PM_{10}, μg/m^3 or mg/kg; ET is the exposure time, 6 h/day; EF is the exposure frequency, 350 days/year; ED is the exposure duration, 6 years for children and 24 years for adults; AT_1 is the average time, for noncarcinogens, $AT_1 = ED$ year × 365 days/year × 24 h/day, and for carcinogens, AT_1 = lifetime year × 365 days/year × 24 h/day (lifetime, 74 years for life expectancy in Henan Province in 2010; http://www.nhfpc.gov.cn/zwgkzt/pwstj/list.shtml); SA is the surface area of skin contacting PM, 2800 cm^2 for children and 3300 cm^2 for adults; AF is the skin adherence factor for PM, 0.2 mg/(cm^2 d); ABS is the absorption fraction, i.e., 0.001 for Cd, 0.03 for As, and 1.0% for other elements (in fact, no values are available for other elements, but 1.0% was hypothesized and used by Hu et al. (2012)); CF is the conversion factor, 10^{-6} kg/mg; BW is the body weight, 15 kg for children (recommended value by the US EPA) and 59 kg for adults (Wang et al., 2009; National Bureau of Statistical of China, 2015); AT_2 is the average time, for noncarcinogens, $AT_2 = ED$ year × 365 days/year, and for carcinogens, AT_2 = lifetime year × 365 days/year (lifetime, i.e., 74 years); and $IngR$ is the ingestion rate, 200 mg/day for children (recommended value by the US EPA) and 50 mg/day for adults (Ministry of Environmental Protection of the People's Republic of China, 2013).

2.5.2. Risk assessment

Carcinogenic and noncarcinogenic effects were evaluated by calculating the carcinogenic risks (CR) and hazard quotient (HQ) posed by toxic elements in $PM_{2.5}$ and PM_{10}, respectively. The relative formulas of the three pathways were expressed as follows:

$$CR_{inhale} = IUR \times EC, \quad (4)$$

$$CR_{dermal} = DAD \times \frac{SF_O}{GIABS}, \quad (5)$$

$$CR_{ingest} = CDI \times SF_O, \quad (6)$$

$$HQ_{inhale} = \frac{EC}{(RfC_i \times 1000\ \mu g/mg)}, \quad (7)$$

$$HQ_{dermal} = \frac{DAD}{RfD_O \times GIABS}, \quad (8)$$

$$HQ_{ingest} = \frac{CDI}{RfD_O}, \quad (9)$$

$$HI = \sum HQ_i, \quad (10)$$

where all parameters used in the formulas were derived from US EPA (2011b; 2011c). IUR is the inhalation unit risk, (μg/m^3)$^{-1}$; SF_O is the Slope Factor, (mg/(kg day))$^{-1}$; $GIABS$ is the gastrointestinal absorption factor; RfC_i is the inhalation reference concentrations, mg/m^3; $RfDo$ is the oral reference dose, mg/(kg day); and hazard index (HI) is the sum of HQ.

3. Results and discussion

3.1. PM mass concentrations

Mass concentrations (from Teflon filters) of $PM_{2.5}$ and PM_{10} are shown in Fig. 2. The daily $PM_{2.5}$ and PM_{10} concentrations ranged from 30 μg/m^3 to 336 μg/m^3 and from 88 μg/m^3 to 495 μg/m^3, respectively. PM exceeded the Chinese National Ambient Air Quality Standards (NAAQS; daily average of 75 μg/m^3 for $PM_{2.5}$ and 150 μg/m^3 for PM_{10}) in 39 and 40 days, accounting for 68% and 70% of the total sampling days for $PM_{2.5}$ and PM_{10}, respectively. The annual mean values of $PM_{2.5}$ (118 ± 63 μg/m^3) and PM_{10} (211 ± 86 μg/m^3) were 2.4 and 2.0 times higher than the NAAQS (annual mean of 35 μg/m^3 for $PM_{2.5}$ and 70 μg/m^3 for PM_{10}). These values are higher than that in Shanghai (two sites: 103 and 149 μg/m^3 in the industrial area and 62 and 97 μg/m^3 in the residential area) (Wang et al., 2013) and Beijing (102 and 149 μg/m^3) (Guo et al., 2010), also much higher than those in the US (42 sites: 2–15 μg/m^3 for $PM_{2.5}$ and 4–21 μg/m^3 for PM_{10}) (Eldred et al., 1997) and Europe (11–30 μg/m^3 for $PM_{2.5}$ and 19–38 μg/m^3 for PM_{10}) (Amato et al., 2016), indicating serious PM pollution in Zhengzhou. PM pollution may be associated with the city construction, and the floor space of buildings under construction is 2.31 × 10^8 m^2 during 2015 in Zhengzhou (Bureau of Statistics of Henan Province, 2016). The average concentrations of $PM_{2.5}$ and PM_{10} decreased in the order of winter (165 ± 84 and 276 ± 97 μg/m^3) > autumn (147 ± 62 and 256 ± 82 μg/m^3) > spring (89 ± 30 and 183 ± 47 μg/m^3) > summer (85 ± 33 and 140 ± 30 μg/m^3). This seasonal concentration variation of PM is attributed to the comprehensive influence of source emissions and meteorological conditions. In winter, extra coal combustion for domestic heating and frequent stagnant meteorological condition contributed to the high PM concentrations.

Moreover, the ratios of $PM_{2.5}/PM_{10}$ are illustrated in Fig. 2. The average seasonal ratios of $PM_{2.5}/PM_{10}$ are 0.54 ± 0.13 (autumn), 0.58 ± 0.18 (winter), 0.51 ± 0.17 (spring), and 0.56 ± 0.14 (summer). The lowest average ratio in spring could be attributed to the high-speed winds and lack of rain in spring in North China (Zhang et al., 2013). The annual ratio of $PM_{2.5}/PM_{10}$ (0.55 ± 0.15) indicated that the fine particulate was the main mass in PM_{10}.

3.2. Chemical composition levels and the difference

3.2.1. WSIIs

The annual mean WSII concentrations of $PM_{2.5}$ and PM_{10} (Table 1) in the study area were 66.1 ± 32.7 and 76.3 ± 38.5 μg/m^3, accounting for 45± 10% and 37± 14% of the total PM respectively. This result showed that WSIIs were found to be the main

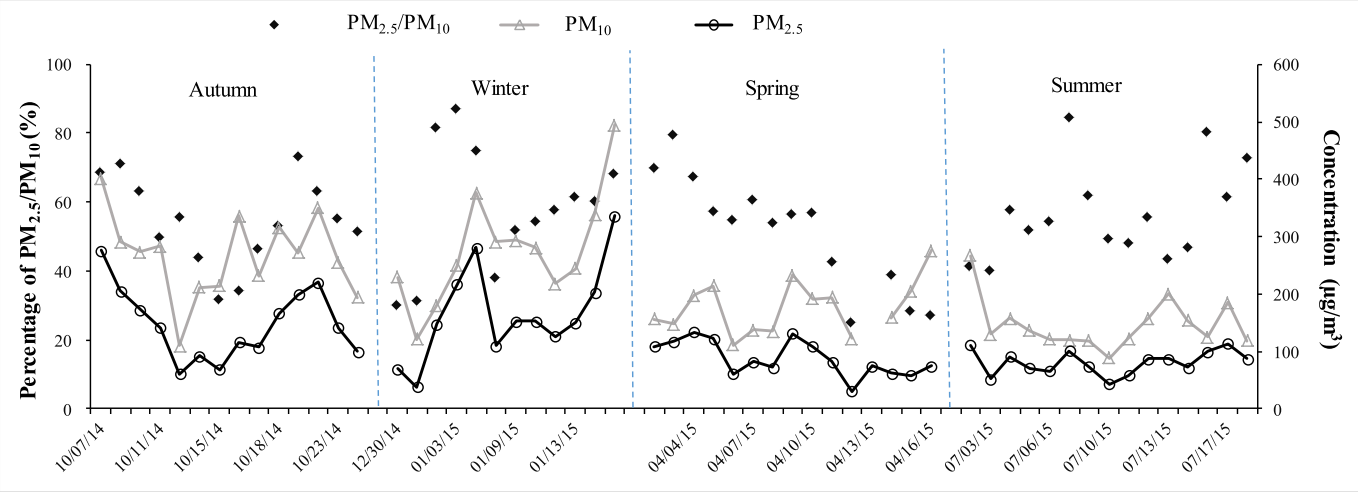

Fig. 2. Variations of mass concentrations of $PM_{2.5}$ and PM_{10} in Zhengzhou from 2014 to 2015.

Table 1
Seasonal average of WSII concentration and ratio of $PM_{2.5}$ and PM_{10}. (a) $PM_{2.5}$ (b) PM_{10}.

	Autumn n = 14	Winter n = 12	Spring n = 16	Summer n = 15	Annual n = 57
$PM_{2.5}$[a] (μg/m^3)	147 ± 62	165 ± 84	89 ± 30	85 ± 33	118 ± 63
WSIIs	54.8 ± 24.3	90.5 ± 48.4	61.6 ± 21.8	58.3 ± 18.0	66.1 ± 32.7
Cl^-	2.6 ± 1.3	7.0 ± 2.6	2.4 ± 1.2	1.6 ± 1.1	3.1 ± 2.5
Ratios					
OC/EC	3.9 ± 0.9	2.1 ± 0.7	2.3 ± 0.4	1.8 ± 0.3	2.4 ± 1.2
NO_3^-/SO_4^{2-}	0.9 ± 0.3	1.1 ± 0.4	1.0 ± 0.3	0.6 ± 0.4	0.9 ± 0.4
WSIIs/$PM_{2.5}$ (%)	37 ± 7	46 ± 7	44 ± 10	53 ± 9	45 ± 10
SIAs/$PM_{2.5}$ (%)	31 ± 8	34 ± 9	35 ± 13	44 ± 11	36 ± 12
OC/$PM_{2.5}$ (%)	14 ± 5	20 ± 6	14 ± 4	12 ± 3	15 ± 6
	Autumn n = 15	Winter n = 12	Spring n = 15	Summer n = 15	Annual n = 57
PM_{10}[a] (μg/m^3)	256 ± 82	276 ± 97	183 ± 47	140 ± 30	211 ± 86
WSIIs	87.5 ± 42.3	101.3 ± 52.9	58.8 ± 26.6	67.9 ± 25.8	76.3 ± 38.5
Cl^-	4.2 ± 3.1	8.8 ± 3.0	2.6 ± 1.1	1.9 ± 1.4	3.8 ± 3.2
Ratios					
OC/EC	4.3 ± 1.6	2.0 ± 0.3	3.1 ± 1.6	2.2 ± 0.3	3.0 ± 2.0
NO_3^-/SO_4^{2-}	1.0 ± 0.3	1.0 ± 0.4	1.1 ± 0.3	0.7 ± 0.3	0.9 ± 0.4
WSIIs/PM_{10} (%)	35 ± 13	37 ± 11	32 ± 14	43 ± 16	37 ± 14
SIAs/PM_{10} (%)	28 ± 13	28 ± 10	26 ± 13	35 ± 16	30 ± 14
OC/PM_{10} (%)	14 ± 6	21 ± 6	11 ± 4	14 ± 4	14 ± 6

SIAs: Secondary Inorganic Aerosols (NH_4^+, NO_3^-, SO_4^{2-}).
WSIIs: 9 water soluble inorganic ions.
[a] The mass concentration of PM was analyzed by Teflon filters.

component of $PM_{2.5}$ and PM_{10} both; however, WSIIs were more concentrated in fine particles than in the coarse fraction. SIAs were the major contributors to WSIIs, and the annual average concentration was 52.5 ± 29.2 μg/m^3 (accounting for approximately 36% of $PM_{2.5}$) and 61.3 ± 34.2 μg/m^3 (accounting for approximately 29% of PM_{10}). SIAs are formed from their gaseous precursors NH_3, SO_2, and NO_x through complicated gas-phase and aqueous-phase chemical reactions. The ratio of SIAs/PM was highest in summer (44% for $PM_{2.5}$ and 35% for PM_{10}), indicating an intense photochemical process in this season.

The concentrations of SO_4^{2-}, NO_3^-, and NH_4^+ in PM are shown in Fig. 3, and the annual concentrations of SIAs follow the order: SO_4^{2-} > NO_3^- > NH_4^+. The seasonal concentrations of SO_4^{2-} were higher in winter (23.5 and 28.9 μg/m^3 for $PM_{2.5}$ and PM_{10}, respectively) and summer (24.2 and 27.2 μg/m^3 for $PM_{2.5}$ and PM_{10}, respectively). One of the reasons is extra coal combustion for resident heating in North China in winter, which increases the emission of the gaseous precursor SO_2. Moreover, a stable atmospheric structure is not in favor of pollutant diffusion in the atmosphere in this season. Another reason is the high conversion rate of SO_2 to PM, which can be attributed to the relatively high humidity and temperature in summer (Yao et al., 2003). The maximum concentration of NO_3^- was measured in winter. NO_3^- levels were related to the synthetic action of various influencing factors, i.e., precursor NO_x emissions, complex photochemical and heterogeneous reactions, and gas–aerosol equilibrium (Zhang et al., 2013). The seasonal average concentration of Cl^- in PM, mainly from coal combustion, garbage burning, and biomass burning emissions, was highest in winter because of a large amount of coal and biomass burned not only for heating but also for cooking in this season.

The mass concentration ratio of NO_3^-/SO_4^{2-} has been used as an indicator of the relative importance of mobile and stationary sources of SO_2 and NO_x (Arimoto et al., 1996; Yao et al., 2002; Xiao and Liu, 2004). The seasonal variation of NO_3^-/SO_4^{2-} in $PM_{2.5}$ and PM_{10} ranged from 0.6 to 1.1 and from 0.7 to 1.1, respectively, with the annual mean of 0.9 ± 0.4, which is higher than the value of 0.6 measured in 2010 at the same site in Zhengzhou (Geng et al., 2013)

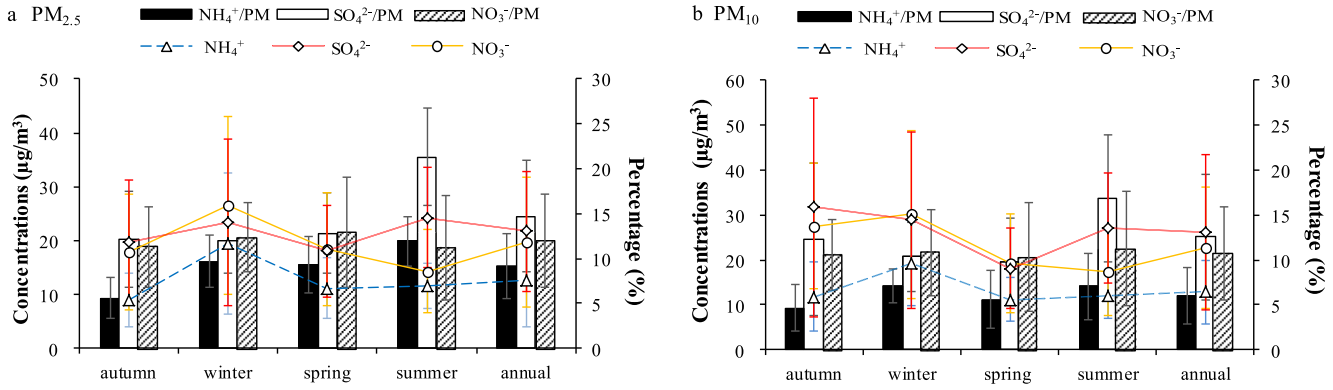

Fig. 3. Seasonal variation of components of SIAs and their ratios in $PM_{2.5}$ and PM_{10} in Zhengzhou.

and higher than that in Shanghai (0.43; Yao et al., 2002), Qingdao (0.35; Hu et al., 2002), and Taiwan (0.20; Fang et al., 2002), but lower than the value of 2.2 measured in Tokyo (Saitoh et al., 2002). Therefore, the contribution of mobile sources is more important than before with the increasing numbers of vehicles.

The cation equivalents (CE) and anion equivalents (AE) in $PM_{2.5}$ and PM_{10} samples were calculated. Base on μeq/m^3 of respective CE and AE for $PM_{2.5}$, the annual average CE/AE ratio was approximately 1.1, with the seasonal ratio in autumn of 0.9 and the other seasonal ratios all approximately 1.2; for PM_{10}, by contrast, the annual and seasonal mean ratios were all 1.3, excluding the value in summer (1.2).

3.2.2. OC and EC levels

OC and EC are also the major components of PM and the daily concentrations are shown in Fig. 4. The annual concentrations of OC in $PM_{2.5}$ and PM_{10} were 22.2 and 32.6 μg/m^3, accounting for 15% and 14%, respectively. EC concentrations were lower, with an annual value of 9.4 μg/m^3 in $PM_{2.5}$ and 12.2 μg/m^3 in PM_{10}. Obvious similar seasonal variations of OC and EC were observed in $PM_{2.5}$ and PM_{10} both, with the highest average concentration in winter, i.e., 37.6 and 17.8 μg/m^3 in $PM_{2.5}$ and 59.3 and 29.9 μg/m^3 in PM_{10}, respectively. Moreover, the ratios of OC/PM were highest in winter, accounting for 20%–21% in $PM_{2.5}$ and PM_{10}, respectively. The lowest average concentration of carbonaceous species was observed in summer (for OC) or autumn (for EC). The seasonality could be related to the variability in emissions and meteorological conditions. The ratio of OC/EC was used to indicate the existence of the secondary organic carbon (SOC). In a previous study, SOC was assumed to exist with ratios exceeding 2.0 to 2.2 (Liu et al., 2016). In this study, SOC was generated by the photochemical process in approximately half of the sampling days.

3.2.3. Element levels

Trace elements play an important role in the estimation of emission source and are associated with the industrial process, traffic, and residential activities. For example, crustal elements, such as Si, Al, Mg, Ca, and Ti, are associated with fugitive dust (Amato et al., 2009). Pb is discharged from the smelting and coal combustion processes (Zhang et al., 2009), and Cd, Mo, Cu, and Ba are generated by vehicle emissions (Garg et al., 2000; Sternbeck et al., 2002; Bozlaker et al., 2013). According to previous reports, element levels in PM exhibited significant differences in different regions. For example, the elements contributed up to 20% for $PM_{2.5}$ in Shanghai during 2009–2010 (Wang et al., 2013). The contribution of total trace elements to the total mass of PM was in the range of 0.4%–0.6% in Navarra during 2009 (Aldabe et al., 2011). The concentration of trace elements in PM is shown in Fig. 5. In this figure, Si was estimated based on the Al–to–Si ratio (0.46 for $PM_{2.5}$ and 0.26 for PM_{10}) (Taylor and Mclennan, 1995; Chow et al., 2015).

In the PM_{10} and $PM_{2.5}$ samples, the relatively high concentrations of trace elements are in the order of Si > Al > Fe > Mg > Zn > Pb > Ti, with 95% (for $PM_{2.5}$) and 98% (for PM_{10}) of total element mass contributions. Crustal elements mainly existed in $PM_{2.5-10}$, and the sum concentration of Si, Al, Fe, Mg, Ti, Ba, and Sr was 18.7 μg/m^3 in PM_{10}, exceeding the value in $PM_{2.5}$ by 2.7 times. However, elements from anthropogenic sources (i.e., Zn, Pb, Cu, As, Cd, and Mo) were more abundant in fine particles than in the coarse fraction.

3.2.4. Mass reconstitution

The material balance, including crustal matter (CM), organic matter (OM), EC, SIAs (i.e., SO_4^{2-}, NO_3^- and NH_4^+), other WSIIs, other elements, and unidentified components, is calculated to understand the contribution of chemical constituents to the total mass of PM (Shen et al., 2014). CM and OM are calculated as follows (Malm et al., 1994; Turpin and Lim, 2001):

$$CM = 2.2 \times [Al] + 2.49 \times [Si] + 1.63 \times [Ca] + 1.94 \times [Ti] + 2.42 \times [Fe], \quad (11)$$

$$OM = 1.6 \times [OC]. \quad (12)$$

According to the chemical composition data and Formulas (11) and (12), the mass closure of $PM_{2.5}$ and PM_{10} in the study area is shown in Fig. 6. The figure shows that the major components are SIAs (a combination of SO_4^{2-}, NO_3^-, and NH_4^+), OM, and CM. SIAs accounts for 36% of $PM_{2.5}$, which is higher than that of PM_{10} (30%). However, the ratio of CM in PM_{10} (31%) is 2.6 times of that in $PM_{2.5}$ (12%), with the highest ratio in spring (14% for $PM_{2.5}$ and 37% for PM_{10}). EC, other WSIIs, and other elements are the minor components, each representing 1%–6% of $PM_{2.5}$ and PM_{10}. This finding indicates that the measures for crust dust prevention and control are more appropriate and effective for decreasing the PM_{10} level than $PM_{2.5}$. Moreover, the appropriate control of precursor gases (i.e., SO_2, NOx and VOCs) can improve $PM_{2.5}$ and PM_{10} pollution, with more success for $PM_{2.5}$.

3.3. Source apportionment of PM_{10} and $PM_{2.5}$

For $PM_{2.5}$, the species OC, EC, NH_4^+, K^+, Ca^{2+}, Cl^-, NO_3^-, SO_4^{2-}, Mg, Al, Si, Ti, V, Mn, Fe, Co, Cu, Zn, As, Cd, Sn, Ba and Pb were classified as

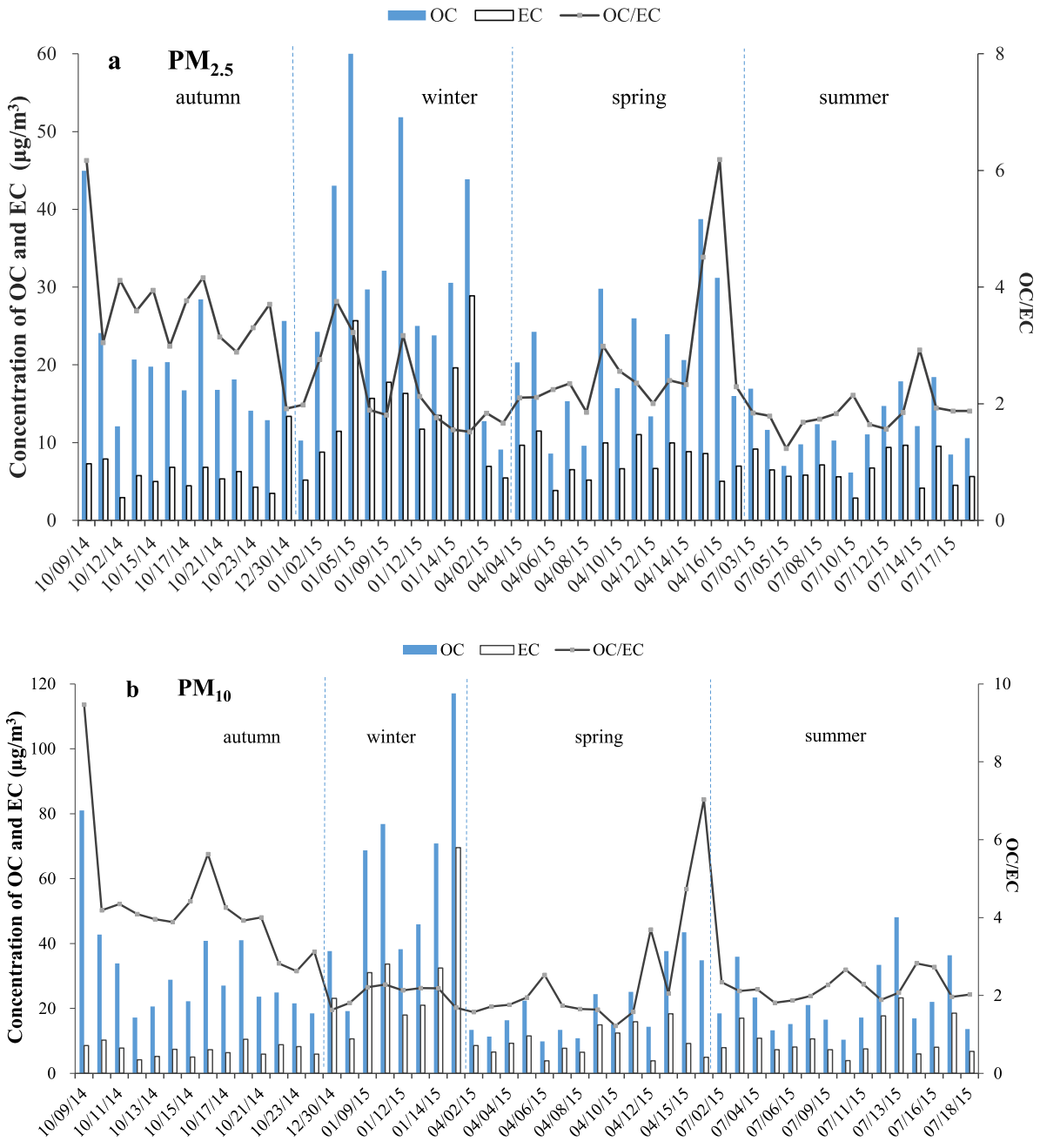

Fig. 4. Concentrations of OC and EC and OC/EC in $PM_{2.5}$ and PM_{10} in Zhengzhou during sampling period.

"strong" variables; Whereas, the species Sr and Ag were categorized "weak" variables, with a tripled uncertainty. "Bad" variables, including Na^+, F^-, B, Se and Mo were excluded from the PMF analysis because the species data don't meet the requirement of analyze input data of PMF 5.0 (US EPA, 2014). For PM_{10}, with no "weak" variables, comparison with $PM_{2.5}$, the differences were the species Na^+, Sr, Ag categorized as "strong" variables. In additional, the species Mg^{2+} was categorized "Bad" because the species Mg was already chosen as "strong" variables. Bootstrap (BS) was run with 100 resamples, recommended value in PMF 5.0 (US EPA, 2014) in the model analysis. The BS uncertainties were interpreted and the number of factors was appropriate because with six factors, all factors for PM, except vehicle factor for fine particle, were mapped above 90% of BS runs (vehicle factor for $PM_{2.5}$ was mapped 81% of runs). Fpeak was used to determine whether a more optimal solution can be found (US EPA, 2014), and the Fpeak strengths, with the values between −3 and 3 were evaluated in this study. The optimal solution of the Base Run was chosen because of an increase of the Q-value due to the Fpeak rotation without optimizing the solution, including comparison of variation of G-space plots, the profiles and contributions. The constrained model was also conducted to optimize the solution, and the constraints for PMF analyses were as follows: for $PM_{2.5}$, the presence of EC in SIAs factor was set to zero; for PM_{10}, the contributions of K and Ca were set to zero in SIAs factor; besides, the contributions of EC specie in SIAs factor, NH_4^+ specie in vehicle and road dust factor, and K specie in dust factor were all pulled down maximally.

As a result, a six–factor solution was chosen for source

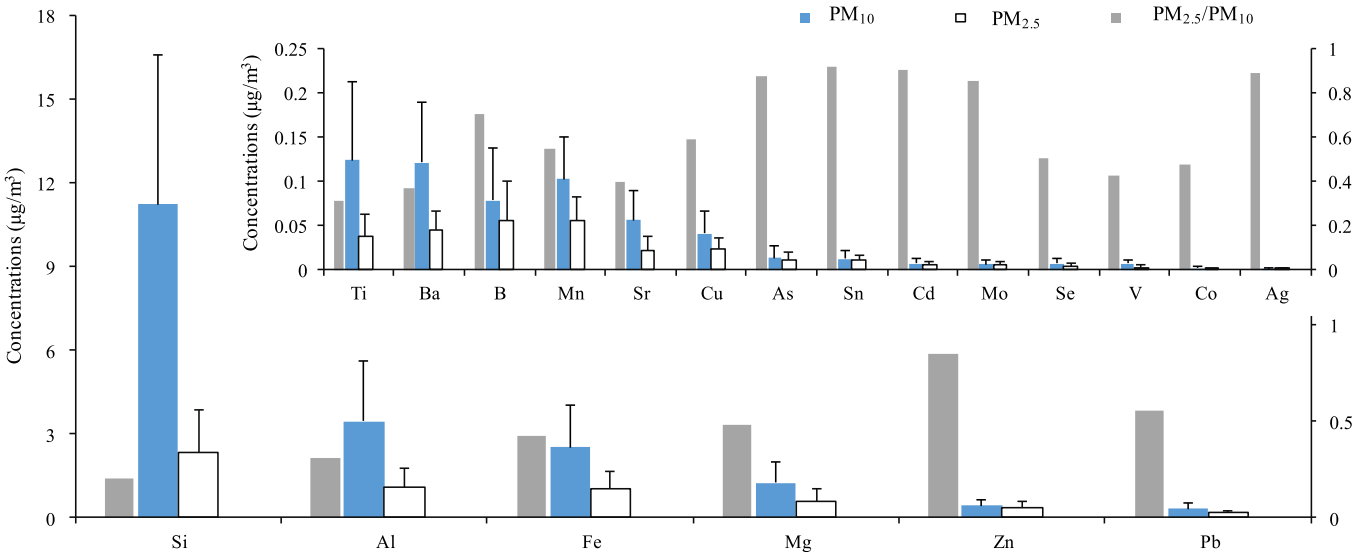

Fig. 5. The annual mean concentrations of trace elements in $PM_{2.5}$ and PM_{10} in Zhengzhou.

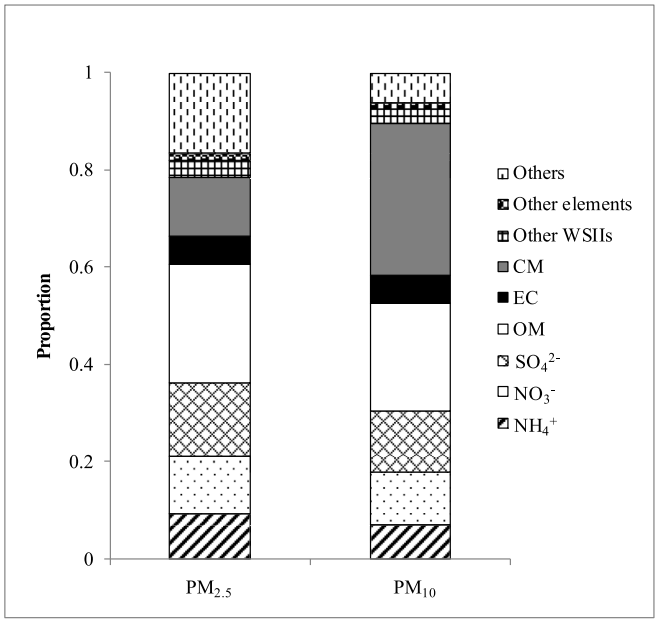

Fig. 6. Mass closure of $PM_{2.5}$ and PM_{10} in Zhengzhou.

apportionment of $PM_{2.5}$ and PM_{10}. The source profiles and source percentage contributions of $PM_{2.5}$ and PM_{10} are illustrated in Figs. 7 and 8, respectively. As main sources of $PM_{2.5}$ and PM_{10}, dust, SIAs, coal combustion, vehicle and road dust, and industry were identified as follows:

Factor 1 is dust source, usually a mix of soil dust, construction dust, demolition dust, and atmospheric dust fall. This source is typically characterized by crustal elements, i.e., Al, Si, Ti, Fe, and Mg. Moreover, OC, Zn, Mn, Sr, Ba, and K^+ exist in this source. This finding is in accordance with the soil dust profile obtained by chemical analyses of resuspended soil samples collected near the site (Jiang et al., 2017a, (accepted for publication)). Similar PM_{10} and $PM_{2.5}$ source profiles for fugitive dust were also presented by Ho et al. (2003) and Kong et al. (2011). Crustal element contents are higher in PM_{10}, consistent with that shown in previous studies (Chan et al., 1997; Li et al., 2004). Fig. 8 shows that dust source has the highest contribution in PM_{10}, with the ratio of 32%, which is 3.3 times of that in $PM_{2.5}$ (10%). This finding indicates that more effective achievement will be gained in decreasing PM_{10} pollution via powerful prevention and control of dust. However, at present, construction and demolition activities are prevalent in the urban areas in Zhengzhou, without effective measures for dust control (Figs. S1 and S2 in the Supplemental Materials). More precise and fine management is needed for the local government to improve PM_{10} pollution.

Factor 2 is SIAs, with remarkable NH_4^+, NO_3^-, and SO_4^{2-} as its representative feature. SIAs are mainly generated by photochemical reaction of precursor gases (i.e., SO_2, NH_3, and NO_x), which are emitted by certain identified sources of human activity (i.e., coal combustion, vehicle, and biomass burning). This source contributes to 26% of $PM_{2.5}$ mass concentration, which is higher than that of PM_{10} (14%). Similar results were obtained by Chan et al. (1997) and Aldabe et al. (2011). This source often has a high content in fine particles; therefore, strict regulatory control of precursor gases is beneficial to reduce the $PM_{2.5}$ level.

Factor 3 is coal combustion, which is represented by high concentrations of Cl^- and is associated with OC, EC, and Pb (Zheng et al., 2005). The highest seasonal concentration of Cl^- (more than twice that of the annual mean value) was observed in winter and this distinctive feature in North China can be attributed to the extra coal consumption for heating. Coal combustion is the predominant source, and its contribution accounts for 24%–25% of $PM_{2.5}$ and PM_{10}, which is only slightly different from that reported by Tian et al. (2016). Coal combustion is the major source of PM in China (Yao et al., 2009), induces locally, regionally, and even globally severe PM pollution (Zhang et al., 2013), and results in aerosol Pb increase (Zhang et al., 2009). Thus, according to the national energy adjustment policy, the reduction of coal consumption, for example, the amount of coal consumption in industrial enterprises above designated size by Zhengzhou in 2015 (33.2 million tons; http://www.ha.stats.gov.cn/hntj/lib/tjnj/2016/indexch.htm) is less than that in 2014 (35.2 million tons; http://www.ha.stats.gov.cn/hntj/lib/tjnj/2015/indexch.htm), is an effective action for improving the PM pollution situation. However, more related

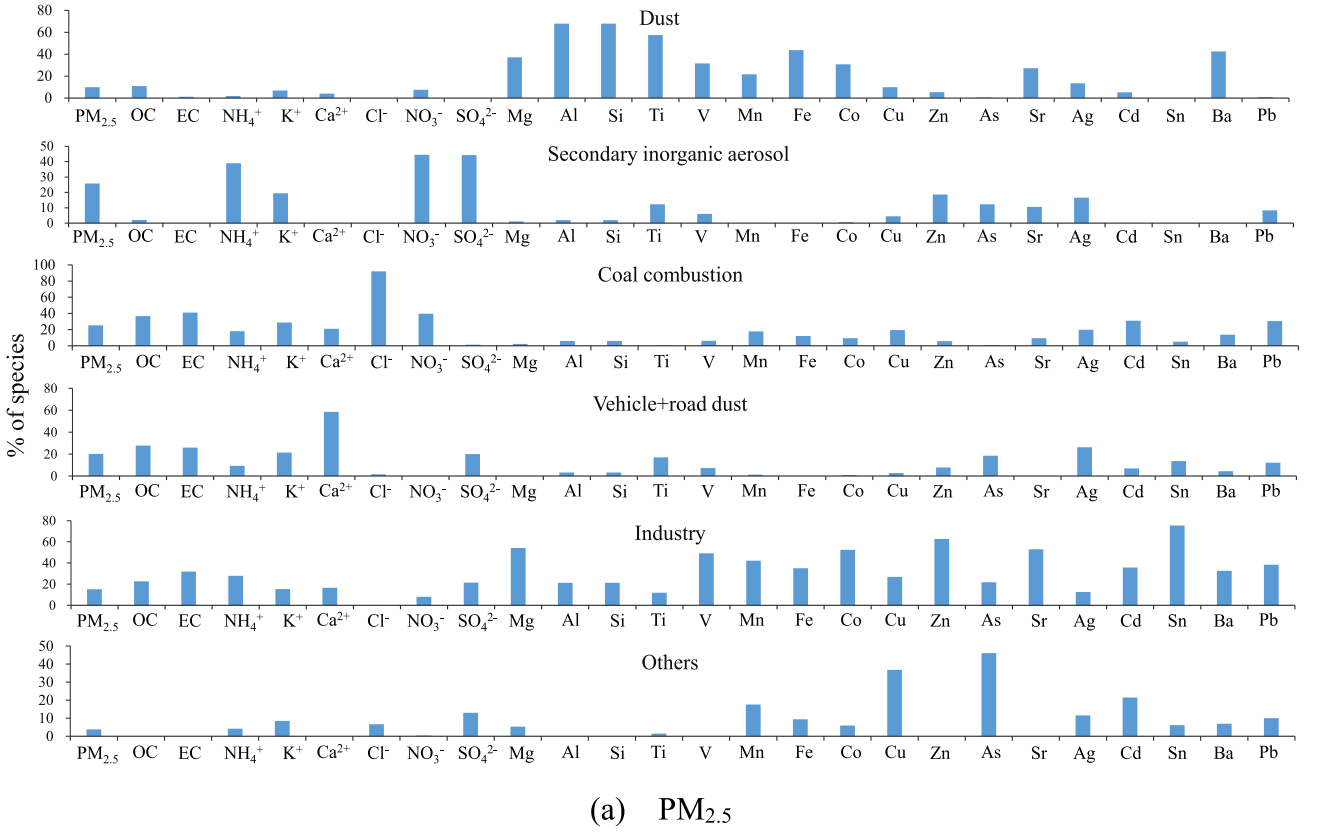

(a) $PM_{2.5}$

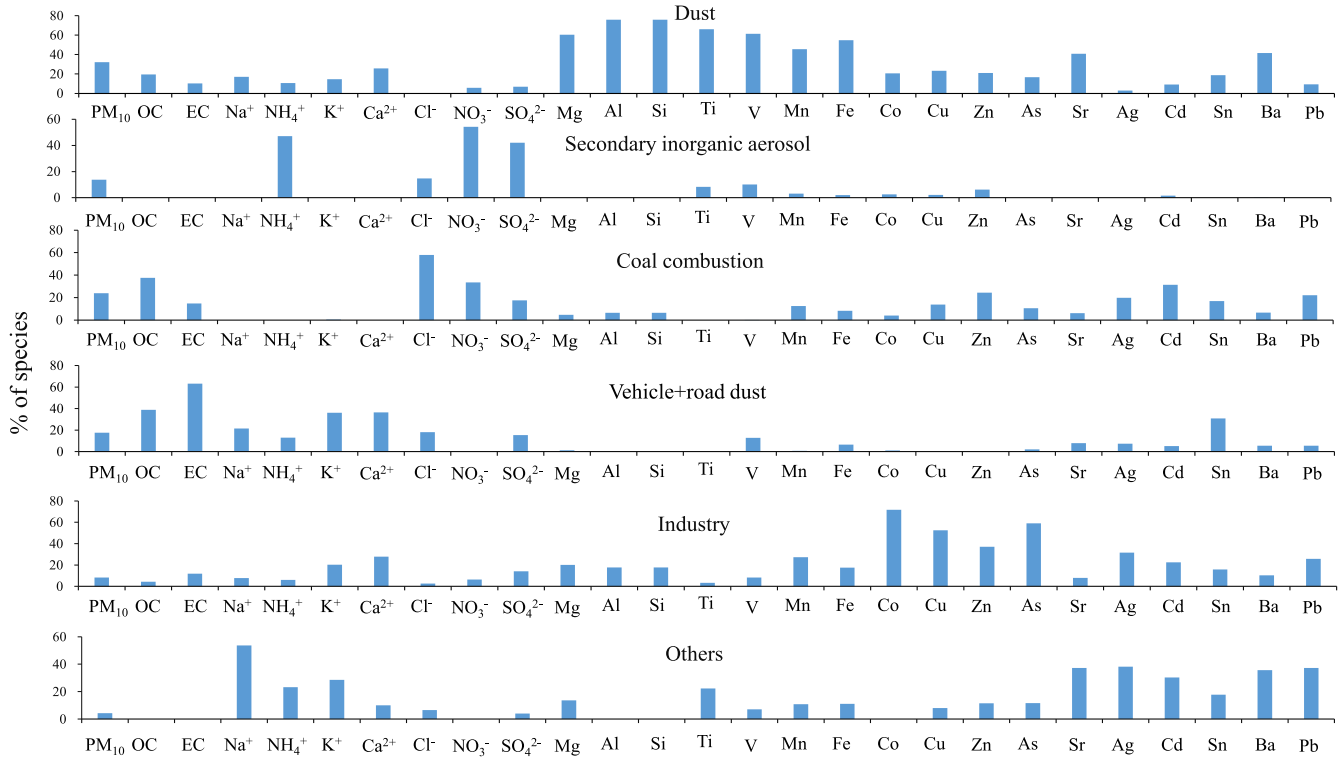

(b) PM_{10}

Fig. 7. Source profiles of $PM_{2.5}$ and PM_{10} based on the PMF model analysis.

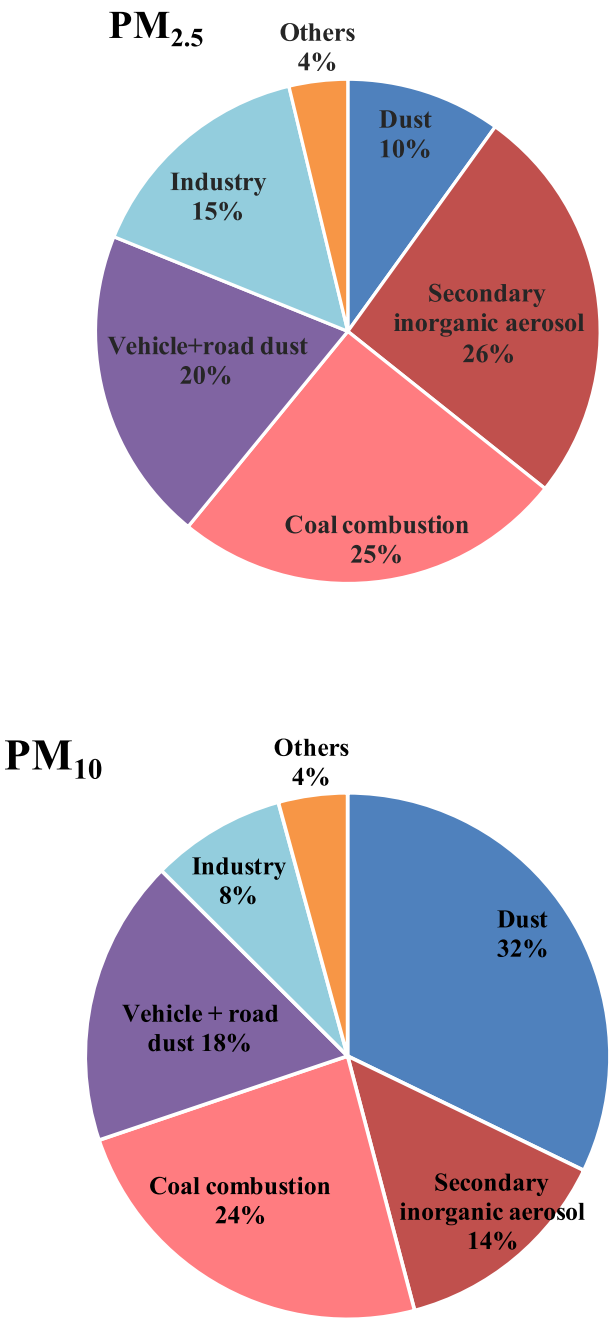

Fig. 8. Source contributions of $PM_{2.5}$ and PM_{10} in Zhengzhou.

efforts should be exerted because of the high levels of $PM_{2.5}$ and PM_{10} in this area.

Factor 4 is mixed source of vehicle and road dust, which is characterized not only by OC, EC, Sn, Ba, Cd, Zn, and Cu but also by Ca^{2+}, K^{+}, and Ti. OC and EC are considered to be tracers of motor vehicle emissions, and EC is an indicator of primary emissions of OC (Yang et al., 2005). EC has a high content, as exhibited by the site close to the west side of 4th Beltway, with numerous heavy–duty diesel trucks. Vehicle–derived metals, Cd, and Cu are discharged from tailpipe emission (Cadle et al., 1999; Sternbeck et al., 2002); Cu, Ba, and Mo are emitted from brake lining and tire tread wear (Garg et al., 2000; Bozlaker et al., 2013); and Zn is identified as the marker of tire wear and brake wear (Furusj et al., 2007). This mixed source contributes 20% to $PM_{2.5}$, which is slightly higher than that of PM_{10} (18%). Moreover, the contribution of vehicle emission alone should have a greater extent in $PM_{2.5}$ because the contribution of dust to PM_{10} is higher than that to $PM_{2.5}$ (Chan et al., 1997; Li et al., 2004). Therefore, with the number of automobiles increasing in recent years, the government should focus more attention on mitigating vehicle emission to alleviate $PM_{2.5}$ contamination in this area.

Factor 5 is industry, with high loads of OC, EC, and elements (i.e., Mn, Co, Fe, Cu, Zn, As, Sn, Cd, and Pb) discharged from the industrial process. Zhang et al. (2013) reported that industrial pollution is one of the vital sources of carbonaceous aerosols, which has been widely ignored. The elements are usually generated by the industrial metal smelting process (Chan et al., 1997; Lim et al., 2010; Dall'Osto et al., 2013). This source contributes 15% and 8% to $PM_{2.5}$ and PM_{10}, respectively.

Factor 6 is unidentified sources, which include biomass burning and account for contributions of only 4%–5% to $PM_{2.5}$ and PM_{10}.

3.4. Health risks posed by toxic elements

Cancer and non-cancer health risk values of toxic elements in $PM_{2.5}$ and PM_{10} through the inhalation, dermal absorption and daily intake pathways are shown in Tables 2–4, respectively. The acceptable or tolerable carcinogenic risk for regulatory purposes is CR between 1×10^{-6} and 1×10^{-4}, and HI < 1 indicates no significant noncarcinogenic risk of the overall elements (US EPA, 2011a). Detailed data on the evaluation of health risks posed by toxic elements in $PM_{2.5}$ and PM_{10} via the three exposure pathways are shown in Tables S1 to S3 in the Supplemental Materials.

Inhalation via mouth and nose is the primary pathway of airborne toxic elements exposure. The carcinogenic risks via inhalation exposure for children and adults to a single element (e.g., Co, As, and Cd) in $PM_{2.5}$ and PM_{10} were all less than 1×10^{-4}, indicating the risk of each element within the acceptable level. Moreover, the integrated carcinogenic risks of these elements in $PM_{2.5}$ and PM_{10} were also within the acceptable level ($<1 \times 10^{-4}$). The noncarcinogenic risks (i.e., HQ) of each element (i.e., As, Cd, Co, V, and Mn) via inhalation exposure were all less than 1, indicating no significant risk. However, the sum of noncarcinogenic risks of the five elements in PM_{10} was 1.27 for children and adults, which is more than the threshold value, indicating significant noncarcinogenic risk of the overall elements.

The CR values of As in $PM_{2.5}$ and PM_{10} through the dermal absorption pathway were between 1.72E-05 and 2.28E-05, indicating the acceptable carcinogenic risk level. The HQ values of each element (i.e., V, Co, Cu, As, Mn, Cd, and Zn) via dermal absorption were also less than 1, with no significant risk. The HI values of the seven elements in $PM_{2.5}$ were 9.15E-01 and 2.74E-01 for children and adults, with no significant risk. The HI values in PM_{10} were higher than those in $PM_{2.5}$, particularly for children (HI > 1), with significant noncarcinogenic risks.

The health risks via the daily intake pathway exist because of the deposition of PM in the atmosphere. The exposure to $PM_{2.5}$ and PM_{10} was investigated as soil and dust exposure via ingestion. The carcinogenic risks of As to children were 2.04E-04 and 2.26E-04 in $PM_{2.5}$ and PM_{10}, respectively, exceeding the acceptable level, indicating that the carcinogenic risk caused by As should be the focus of more attention. The carcinogenic risks of As to adults were 5.19E-05 and 5.75E-05 in $PM_{2.5}$ and PM_{10}, implying potential acceptable carcinogenic risk. Notably, the noncarcinogenic risks of As and Cd in $PM_{2.5}$ and PM_{10} to children were significant, with HQ all higher than 1. Moreover, the noncarcinogenic risks of As were more important, with HQ values of 5.60 in $PM_{2.5}$ and 6.20 in PM_{10}. For adults, neither HQ of each element nor HI of the seven elements

Table 2
Cancer and non-cancer health risk values of toxic elements in $PM_{2.5}$ and PM_{10} through the inhalation pathway.

Toxic elements	$PM_{2.5}$				PM_{10}			
	Carcinogenic risk		Non-Carcinogenic risk		Carcinogenic risk		Non-Carcinogenic risk	
	Children	Adults	Children	Adults	Children	Adults	Children	Adults
V			1.01E-02	1.01E-02			2.02E-02	2.02E-02
Co	1.22E-07	4.90E-07	2.80E-02	2.80E-02	6.50E-07	2.60E-06	1.48E-01	1.48E-01
As	1.30E-06	5.18E-06	2.48E-01	2.48E-01	1.44E-06	5.74E-06	2.74E-01	2.74E-01
Mn			3.15E-01	3.15E-01			5.55E-01	5.55E-01
Cd	3.60E-07	1.44E-06	2.47E-01	2.47E-01	3.97E-07	1.59E-06	2.72E-01	2.72E-01
HI			8.48E-01	8.48E-01			1.27E+00	1.27E+00

Table 3
Cancer and non-cancer health risk values of toxic elements in $PM_{2.5}$ and PM_{10} through the dermal absorption pathway.

Toxic elements	$PM_{2.5}$				PM_{10}			
	Carcinogenic risk		Non-Carcinogenic risk		Carcinogenic risk		Non-Carcinogenic risk	
	Children	Adults	Children	Adults	Children	Adults	Children	Adults
V			9.80E-02	2.94E-02			1.97E-01	5.90E-02
Co			7.08E-03	2.12E-03			3.76E-02	1.13E-02
Cu			2.18E-03	6.52E-04			3.63E-03	1.09E-03
As	1.72E-05	2.06E-05	4.70E-01	1.41E-01	1.90E-05	2.28E-05	5.21E-01	1.56E-01
Mn			2.08E-01	6.23E-02			3.66E-01	1.10E-01
Cd			1.25E-01	3.75E-02			1.38E-01	4.13E-02
Zn			4.28E-03	1.28E-03			4.87E-03	1.46E-03
HI			9.15E-01	2.74E-01			1.27E+00	3.80E-01

Table 4
Cancer and non-cancer health risk values of toxic elements in $PM_{2.5}$ and PM_{10} through the daily intake pathway.

Toxic elements	$PM_{2.5}$				PM_{10}			
	Carcinogenic risk		Non-Carcinogenic risk		Carcinogenic risk		Non-Carcinogenic risk	
	Children	Adults	Children	Adults	Children	Adults	Children	Adults
V			9.10E-02	5.78E-03			1.83E-01	1.16E-02
Co			2.53E-01	1.61E-02			1.34E+00	8.53E-02
Cu			7.77E-02	4.94E-03			1.30E-01	8.24E-03
As	2.04E-04	5.19E-05	5.60E+00	3.56E-01	2.26E-04	5.75E-05	6.20E+00	3.94E-01
Mn			2.97E-01	1.89E-02			5.23E-01	3.32E-02
Cd			1.12E+00	7.09E-02			1.23E+00	7.82E-02
Zn			1.53E-01	9.72E-03			1.74E-01	1.11E-02
HI			7.59E+00	4.82E-01			9.78E+00	6.22E-01

(i.e., V, Co, Cu, As, Mn, Cd, and Zn) were all less than 1, with no significant risk.

4. Conclusions

In this study, $PM_{2.5}$ and PM_{10} samples were collected in Zhengzhou, and their characteristics of mass concentration, chemical composition, source apportionment and health risks of toxic elements were analyzed. The annual mean values of $PM_{2.5}$ (118 ± 63 μg/m^3) and PM_{10} (211 ± 86 μg/m^3) were 2.4 and 2.0 times higher than the NAAQS, indicating serious PM pollution in the study area. The highest average concentrations of $PM_{2.5}$ and PM_{10} were in winter, probably caused by extra coal combustion for domestic heating and frequent stagnant meteorological condition.

WSIIs were the main component of PM, accounting for 45± 10% of $PM_{2.5}$ and 37 ± 14% of PM_{10}, and were more concentrated in fine particles. SIAs were the major contributors to WSIIs, and the ratio of SIAs/PM was highest in summer (44% for $PM_{2.5}$ and 35% for PM_{10}), indicating an intense photochemical process. The seasonal concentrations of SO_4^{2-} were higher in winter and summer because of the variation of emissions and atmospheric conditions. The ratio of NO_3^-/SO_4^{2-} implied that the contribution of mobile sources is more important than before. The annual concentration of OC accounted for 14%–15% in $PM_{2.5}$ and PM_{10}, and SOC was generated by the photochemical process in approximately half of the sampling days. Crustal elements mainly existed in $PM_{2.5-10}$; however, elements from anthropogenic sources (i.e., Zn, Pb, Cu, As, Cd, and Mo) were abundant in fine particles than in the coarse fraction.

The source apportionment showed that dust, SIAs, coal combustion, vehicle and road dust, and industry were the main pollution sources, accounting for 10%, 26%, 25%, 20%, and 15% in $PM_{2.5}$ and 32%, 14%, 24%, 18% and 8% in PM_{10}, respectively. The different source contributions were found in PM_{10} and $PM_{2.5}$. Dust source has the highest contribution in PM_{10}, indicating that more effective achievement will be gained in decreasing PM_{10} pollution via powerful prevention and control of dust. SIAs source has the highest content in fine particles; therefore, strict regulatory control of the precursor gases is beneficial to reduce the $PM_{2.5}$ level. The reduction of coal consumption and proper control measures on vehicle emission are effective actions for improving the $PM_{2.5}$ and PM_{10} pollution situation, and more related efforts should be exerted.

The carcinogenic risks of As to children through the daily intake pathway in $PM_{2.5}$ and PM_{10} exceeded the acceptable level,

indicating the need for more investigation. Other cancer health risks for children or adults through the three pathways were all tolerable. Noncarcinogenic risks of As and Cd in $PM_{2.5}$ and PM_{10} to children via the daily intake pathway were significant. Moreover, the sum of noncarcinogenic risks in PM_{10} via inhalation exposure for local residents and that via dermal absorption for children were significant.

Acknowledgment

The study was supported by Public Welfare Project from Ministry of Environmental Protection of the People's Republic of China (grant no. 201409010) and Central Leading Local Development of Science and Technology Project in China (grant no. HN 2016-149).

Appendix A. Supplementary data

Supplementary data related to this article can be found at https://doi.org/10.1016/j.apr.2017.07.005.

References

Amato, F., Alastuey, A., Karanasiou, A., Lucarelli, F., Nava, S., Calzolai, G., Severi, M., Becagli, S., Gianelle, V.L., Colombi, C., Alves, C., Custódio, D., Nunes, T., Cerqueira, M., Pio, C., Eleftheriadis, K., Diapouli, E., Reche, C., Minguillón, M.C., Manousakas, M.-I., Maggos, T., Vratolis, S., Harrison, R.M., Querol, X., 2016. AIRUSE-LIFE+: a harmonized PM speciation and source apportionment in five southern European cities. Atmos. Chem. Phys. 16, 3289–3309.

Amato, F., Pandolfi, M., Viana, M., Querol, X., Alastuey, A., Moreno, T., 2009. Spatial and chemical patterns of PM_{10} in road dust deposited in urban environment. Atmos. Environ. 43, 1650–1659.

Arimoto, R., Duce, R.A., Savoie, D.L., Prospero, J.M., Talbot, R., Cullen, J.D., Tomza, U., Lewis, N.F., Ray, B.J., 1996. Relationships among aerosol constituents from Asia and the North Pacific during Pem-West A. J. Geophys. Res. 101, 2011–2023.

Aldabe, J., Elustondo, D., Santamaría, C., Lasheras, E., Pandolfi, M., Alastuey, A., Querol, X., Santamaría, J.M., 2011. Chemical characterisation and source apportionment of $PM_{2.5}$ and PM_{10} at rural, urban and traffic sites in Navarra (North of Spain). Atmos. Res. 102, 191–205.

Bozlaker, A., Spada, N.J., Fraser, M.P., Chellam, S., 2013. Elemental characterization of $PM_{2.5}$ and PM_{10} emitted from light duty vehicles in the Washburn Tunnel of Houston, Texas: release of rhodium, palladium, and platinum. Environ. Sci. Technol. 48, 54–62.

Brown, S.G., Eberly, S., Paatero, P., Norris, G.A., 2015. Methods for estimating uncertainty in PMF solutions: examples with ambient air and water quality data and guidance on reporting PMF results. Sci. Total Environ. 518, 626–635.

Bureau of Statistics of Henan Province, 2016. In: Henan Statistical Yearbook 2016. China Statistics Press, Beijing (in Chinese).

Bytnerowicz, A., Omasa, K., Paolletti, E., 2007. Integrated effects of air pollution and climate change on forest: a northern hemisphere perspective. Environ. Pollut. 147, 438–445.

Cadle, S.H., Mulawa, P.A., Hunsanger, E.C., Nelson, K., Ragazzi, R.A., Barrett, R., Gallagher, G.L., Lawson, D.R., Knapp, K.T., Snow, R., 1999. Composition of light-duty motor vehicle exhaust particulate matter in the Denver, Colorado Area. Environ. Sci. Technol. 33, 2328–2339.

Cesari, D., Donateo, A., Conte, M., Contini, D., 2016. Inter-comparison of source apportionment of PM_{10}, using PMF and CMB in three sites nearby an industrial area in central Italy. Atmos. Res. 182, 282–293.

Chan, Y.C., Simpson, R.W., Mctainsh, G.H., Vowles, P.D., Cohen, D.D., Bailey, G.M., 1997. Characterisation of chemical species in $PM_{2.5}$ and PM_{10} aerosols in Brisbane, Australia. Atmos. Environ. 31, 3773–3785.

Chan, C.K., Yao, X., 2008. Air pollution in mega cities in China. Atmos. Environ. 42, 1–42.

Cheng, S.H., Yang, L.X., Zhou, X.H., Xue, L.K., Gao, X.M., Zhou, Y., Wang, W.X., 2011. Size-fractionated water-soluble ions, situ PH and water content in aerosol on hazy days and the influences on visibility impairment in Jinan, China. Atmos. Environ. 45, 4631–4640.

Chow, J.C., Lowenthal, D.H., Chen, L.W.A., Wang, X., Watson, J.G., 2015. Mass reconstruction methods for $PM_{2.5}$: a review. Air Qual. Atmos. Hlth 8, 243–263.

Dall'Osto, M., Querol, X., Amato, F., Karanasiou, A., Lucarelli, F., Nava, S., Calzolai, G., Chiari, M., 2013. Hourly elemental concentrations in $PM_{2.5}$ aerosols sampled simultaneously at urban background and road site during SAPUSS – diurnal variations and PMF receptor modelling. Atmos. Chem. Phys. 13, 4375–4392.

Eldred, R.A., Cahill, T.A., Flocchini, R.G., 1997. Composition of $PM_{2.5}$ and PM_{10} aerosols in the IMPROVE network. J. Air Waste Manage 47, 194–203.

Fang, G., Chang, C., Wu, Y., Fu, P.P., Yang, C., Chen, C., Chang, S., 2002. Ambient suspended particulate matters and related chemical species study in central Taiwan, Taichung during 1998–2001. Atmos. Environ. 36, 1921–1928.

Fu, Q.Y., Zhuang, G.S., Wang, J., Xu, C., Huang, K., Li, J., Hou, B., Lu, T., Streets, D.G., 2008. Mechanism of formation of the heaviest pollution episode ever recorded in the Yangtze River Delta, China. Atmos. Environ. 42, 2023–2036.

Furusj, E., Sternbeck, J., Cousins, A.P., 2007. PM_{10} source characterization at urban and highway roadside locations. Sci. Total Environ. 387, 206–219.

Gao, J., Tian, H., Cheng, K., Lu, L., Zheng, M., Wang, S., Hao, J., Wang, K., Hua, S., Zhu, C., Wang, Y., 2015. The variation of chemical characteristics of $PM_{2.5}$ and PM_{10} and formation causes during two haze pollution events in urban Beijing, China. Atmos. Environ. 107, 1–8.

Garg, B.D., Cadle, S.H., Mulawa, P.A., Groblicki, P.J., Laroo, C., Parr, G.A., 2000. Brake wear particulate matter emissions. Environ. Sci. Technol. 34, 4463–4469.

Geng, N.B., Wang, J., Xu, Y.F., Zhang, W.D., Chen, C., Zhang, R.Q., 2013. $PM_{2.5}$ in an industrial district of Zhengzhou, China: chemical composition and source apportionment. Particuology 11, 99–109.

Guo, Y.M., Tong, S.L., Zhang, Y.S., Barnett, A.G., Jia, Y.P., Pan, X.C., 2010. The relationship between particulate air pollution and emergency hospital visits for hypertension in Beijing. China. Sci. Total Environ. 408, 4446–4450.

Ho, K.F., Lee, S.C., Chow, J.C., Watson, J.G., 2003. Characterization of PM_{10} and $PM_{2.5}$ source profiles for fugitive dust in Hong Kong. Atoms. Environ. 37, 1023–1032.

Hu, M., He, L., Zhang, Y., Wang, M., Kim, Y.P., Moon, K.C., 2002. Seasonal variation of ionic species in fine particles at Qingdao, China. Atoms. Environ. 36, 5853–5859.

Hu, X., Zhang, Y., Ding, Z.H., Wang, T.J., Lian, H.Z., Sun, Y.Y., Wu, J.C., 2012. Bioaccessibility and health risk of arsenic and heavy metals (Cd, Co, Cr, Cu, Ni, Pb, Zn and Mn) in TSP and $PM_{2.5}$ in Nanjing, China. Atmos. Environ. 57, 146–152.

Jang, E., Alam, M.S., Harrison, R.M., 2013. Source apportionment of polycyclic aromatic hydrocarbons in urban air using positive matrix factorization and spatial distribution analysis. Atmos. Environ. 79, 271–285.

Jiang, N., Dong, Z., Xu, Y.Q., Yu, F., Yin, S.S., Zhang, R.Q., Tang, X.Y., 2017a. Characterization of $PM_{10}$and $PM_{2.5}$ source profiles of fugitive dust in Zhengzhou, China. Aerosol Air Qual. Res. (accepted for publication) http://aaqr.org/article/detail/AAQR-17-04-OA-0132.

Jiang, N., Li, Q., Su, F.C., Wang, Q., Yu, X., Kang, P.R., Zhang, R.Q., Tang, X.Y., 2017b. Chemical characteristics and source apportionment of $PM_{2.5}$, between heavily polluted days and other days in Zhengzhou, China. J. Environ. Sci. https://doi.org/10.1016/j.jes.2017.05.006.

Kang, C.M., Lee, H.S., Kang, B.W., Lee, S.K., Sunwoo, Y., 2004. Chemical characteristics of acidic gas pollutants and $PM_{2.5}$ species during hazy episodes in Seoul, South Korea. Atmos. Environ. 38, 4749–4760.

Kassomenos, P.A., Vardoulakis, S., Chaloulakou, A., Paschalidou, A.K., Grivas, G., Borge, R., Lumbrerasd, J., 2014. Study of PM_{10}, and $PM_{2.5}$ levels in three European cities: analysis of intra and inter urban variations. Atmos. Environ. 87, 153–163.

Kong, S.F., Ji, Y.Q., Lu, B., Chen, L., Han, B., Li, Z.Y., Bai, Z.P., 2011. Characterization of PM_{10} source profiles for fugitive dust in Fushun-a city famous for coal. Atmos. Environ. 45, 5351–5365.

Lai, S., Zhao, Y., Ding, A., Zhang, Y., Song, T., Zheng, J., Ho, K.F., Lee, S.-c., Zhong, L., 2016. Characterization of $PM_{2.5}$ and the major chemical components during a 1-year campaign in rural Guangzhou, Southern China. Atmos. Res. 167, 208–215.

Li, Z., Hopke, P.K., Husain, L., Qureshi, S., Dutkiewicz, V.A., Schwab, J.J., Drewnick, F., Demerjian, K.L., 2004. Sources of fine particle composition in New York City. Atmos. Environ. 38, 6521–6529.

Lim, J.M., Lee, J.H., Moon, J.H., Chung, Y.S., Kim, K.H., 2010. Source apportionment of PM_{10} at a small industrial area using positive matrix factorization. Atmos. Res. 95, 88–100.

Liu, B.S., Song, N., Dai, Q.L., Mei, R.B., Sui, B.H., Bi, X.H., Feng, Y.C., 2016. Chemical composition and source apportionment of ambient $PM_{2.5}$ during the non-heating period in Taiwan, China. Atmos. Res. 170, 23–33.

Malm, W.C., Sisler, J.F., Huffman, D., Eldred, R.A., Cahill, T.A., 1994. Spatial and seasonal trends in particle concentration and optical extinction in the United States. J. Geophys. Res. Atmos. 99, 1347–1370.

Manousakas, M., Papaefthymiou, H., Diapouli, E., Migliori, A., Karydas, A., Radović, B., Eleftheriadis, K., 2016. Assessment of $PM_{2.5}$ sources and their corresponding level of uncertainty in a coastal urban area using EPA PMF 5.0 enhanced diagnostics. Sci. Total Environ. 574, 155–164.

Ministry of Environmental Protection of the People's Republic of China, 2013. Exposure Factors Handbook of Chinese Population. China Environmental Press, Beijing (in Chinese).

Moosmüller, H., Chakrabarty, R.K., Arnott, W.P., 2009. Aerosol light absorption and its measurement: a review. J. Quant. Spectrosc. Radiat. Transf. 110, 844–878.

National Bureau of Statistical of China, 2015. In: China Statistical Yearbook 2015. China Statistics Press, Beijing (in Chinese).

Paatero, P., Tapper, U., 1994. Positive matrix factorization: a non-negative factor model with optimal utilization of error estimates of data values. Environmetrics 5, 111–126.

Putaud, J.P., Van Dingenen, R., Alastuey, A., Bauer, H., Birmili, W., Cyrys, J., Flentje, H., Fuzzi, S., Gehrig, R., Hansson, H.C., Harrison, R.M., Herrmann, H., Hitzenberger, R., Hüglin, C., Jones, A.M., Kasper-Giebl, A., Kiss, G., Kousa, A., Kuhlbusch, T.A.J., Löschau, G., Maenhaut, W., Molnar, A., Moreno, T., Pekkanen, J., Perrino, C., Pitz, M., Pusbaum, H., Querol, X., Rodriguez, S., Salma, I., Schwarz, J., Smolik, J., Scheneider, J., Spindler, G., Ten Brink, H., Tursic, J., Viana, M., Wiedensohler, A., Raes, F., 2010. A European aerosol phenomenology-3: physical and chemical characteristics of particulate matter from 60 rural, urban, and kerbside sites across Europe. Atmos. Environ. 44, 1308–1320.

Querol, X., Viana, M., Alastuey, A., Amato, F., Moreno, T., Castillo, S., Pey, J., de la Rosa, J., Sánchez de la Campa, A., Artiñano, B., Salvador, P., García dos Santos, S.,

Fernández-Patier, R., Moreno-Grau, S., Negral, L., Minguillón, M.C., Monfort, E., Gil, J.I., Inza, A., Ortega, L.A., Santamaría, J.M., Zabalza, J., 2007. Source origin of trace elements in PM from regional background, urban and industrial sites of Spain. Atmos. Environ. 41, 7219–7231.

Saitoh, K., Sera, K., Hirano, K., Shirai, T., 2002. Chemical characterization of particles in winter-night smog in Tokyo. Atmos. Environ. 36, 435–440.

Shen, G.F., Xue, M., Yuan, S.Y., Zhang, J., Zhao, Q.Y., Li, B., Wu, H.S., Ding, A.J., 2014. Chemical compositions and reconstructed light extinction coefficients of particulate matter in a mega-city. in the western Yangtze River Delta, China. Atmos. Environ. 83, 14–20.

Shen, R., Schäfer, K., Schnelle-Kreis, J., Shao, L., Norra, S., Kramar, U., Michalke, B., Abbaszade, G., Streibel, T., Fricker, M., Chen, Y., 2016. Characteristics and sources of PM in seasonal perspective – a case study from one year continuously sampling in Beijing. Atmos. Pollut. Res. 7, 235–248.

Sternbeck, J., Åke Sjödin, Andréasson, K., 2002. Metal emissions from road traffic and the influence of resuspension—results from two tunnel studies. Atmos. Environ. 36, 4735–4744.

Tan, J.H., Duan, J.C., He, K.B., Ma, Y.L., Duan, F.K., Chen, Y., Fu, J.M., 2009. Chemical characteristics of $PM_{2.5}$ during a typical haze episode in Guangzhou. J. Environ. Sci. 21, 774–781.

Tauler, R., Viana, M., Querol, X., Alastuey, A., Flight, R.M., Wentzell, P.D., Hopke, P.K., 2009. Comparison of the results obtained by four receptor modelling methods in aerosol source apportionment studies. Atmos. Environ. 43, 3989–3997.

Taylor, S.R., Mclennan, S.M., 1995. The geochemical evolution of the continental crust. Rev. Geophys. 33, 293–301.

Tian, Y.Z., Shi, G.L., Huang-fu, Y.Q., Song, D.L., Liu, J.Y., Zhou, L.D., Feng, Y.C., 2016. Seasonal and regional variations of source contributions for PM_{10} and $PM_{2.5}$ in urban environment. Sci. Total Environ. 557–558, 697–704.

Turpin, B.J., Lim, H.J., 2001. Species contributions to $PM_{2.5}$ mass concentrations Revisiting common assumptions for estimating organic mass. Aerosol. Sci. Tech. 35, 602–610.

US EPA, 2011a. Risk assessment guidance for superfund. In: Part a: Human Health Evaluation Manual; Part E, Supplemental Guidance for Dermal Risk Assessment; Part F, Supplemental Guidance for Inhalation Risk Assessment, vol. I. http://www.epa.gov/oswer/riskassessment/human_health_exposure.htm.

US EPA, 2011b. The screening level (RSL) Tables (last updated June 2011). Available on-line at: http://www.epa.gov/region9/superfund/prg/index.html.

US EPA, 2011c. User's guide and background technical document for US EPA region 9's Preliminary remediation goals (PRG) table. http://www.epa.gov/reg3hwmd/risk/human/rb-concentrationtable/usersguide.htm.

US EPA, 2014. Positive Matrix Factorization (PMF) 5.0 Fundamentals and User Guide. Office of Research and Development, Washington, DC. https://www.epa.gov/sites/production/files/2015-02/documents/pmf_5.0_user_guide.pdf.

US EPA, 2016. Definition and Procedure for the Determination of the Method Detection Limit, Revision 2. Office of Science and Technology, Washington, DC. In: https://www.epa.gov/sites/production/files/2016-12/documents/mdl-procedure_rev2_12-13-2016.pdf.

Wang, J., Hu, Z., Chen, Y., Chen, Z., Xu, S., 2013. Contamination characteristics and possible sources of PM_{10} and $PM_{2.5}$ in different functional areas of Shanghai, China. Atmos. Environ. 68, 221–229.

Wang, J., Li, X., Jiang, N., Zhang, W., Zhang, R., Tang, X., 2015. Long term observations of PM $_{2.5}$-associated PAHs: comparisons between normal and episode days. Atmos. Environ. 104, 228–236.

Wang, Q., Jiang, N., Yin, S.S., Li, X., Yu, F., Guo, Y., Zhang, R.Q., 2017. Carbonaceous species in $PM_{2.5}$, and PM_{10}, in urban area of Zhengzhou in China: seasonal variations and source apportionment. Atmos. Res. 191, 1–11.

Wang, X.F., Wang, W.X., Yang, L.X., Gao, X.M., Nie, W., Yu, Y.C., Xu, P., Zhou, Y., Wang, Z., 2012. The secondary formation of inorganic aerosols in the droplet mode through heterogeneous aqueous reactions under haze conditions. Atmos. Environ. 63, 68–76.

Wang, Z.S., Duan, X.L., Liu, P., Nie, J., Huang, N., Zhang, J.L., 2009. Human exposure factors of Chinese people in environmental health risk assessment. Res. Environ. Sci. 22, 1164–1170 (in Chinese).

Xiao, H., Liu, C., 2004. Chemical characteristics of water soluble components in TSP over Guiyang, SW China, 2003. Atmos. Environ. 38, 6297–6306.

Yang, F., He, K., Ye, B., Chen, X., Cha, L., Cadle, S.H., Chan, T., Mulawa, P.A., 2005. One year record of organic and elemental carbon in fine particles in downtown Beijing and Shanghai. Atmos. Chem. Phys. 5, 1449–1457.

Yao, Q., Li, S.Q., Xu, H.W., Zhuo, J.K., Song, Q., 2009. Studies on formation and control of combustion particulate matter in China: a review. Energy 34, 1296–1309.

Yao, X.H., Chan, C.K., Fang, M., Cadle, S., Chan, T., Mulawa, P., He, K.B., Ye, B.M., 2002. The water-soluble ionic composition of $PM_{2.5}$ in Shanghai and Beijing, China. Atmos. Environ. 36, 4223–4234.

Yao, X., Lau, A.P.S., Fang, M., Chan, C.K., Hu, M., 2003. Size distribution and formation of ionic species in atmospheric particulate pollutants in Beijing, China. Atmos. Environ. 37, 2991–3000.

Ye, B.M., Ji, X.L., Yang, H.Z., Yao, X.H., Chan, C.K., Cadle, S.H., Chan, T., Mulawa, P.A., 2003. Concentration and chemical composition of $PM_{2.5}$ in Shanghai for a 1-year period. Atmos. Environ. 37, 499–510.

Yin, J., Harrison, R.M., 2008. Pragmatic mass closure study for PM_1, $PM_{2.5}$ and PM_{10} at roadside, urban background and rural sites. Atmos. Environ. 42, 980–988.

Yu, F., Yan, Q., Jiang, N., Su, F., Zhang, L., Yin, S., Li, Y., Zhang, R., 2016. Tracking pollutant characteristics during haze events at background site Zhongmu, Henan province, China. Atmos. Pollut. Res. 8, 64–73.

Zhang, R., Jing, J., Tao, J., Hsu, S.C., Wang, G., Cao, J., Lee, C.S.L., Zhu, L., Chen, Z., Zhao, Y., Shen, Z., 2013. Chemical characterization and source apportionment of $PM_{2.5}$ in Beijing: seasonal perspective. Atmos. Chem. Phys. 13, 7053–7074.

Zhang, Y., Wang, X., Chen, H., Yang, X., Chen, J., Allen, J.O., 2009. Source apportionment of lead-containing aerosol particles in shanghai using single particle mass spectrometry. Chemosphere 74, 501–507.

Zheng, M., Salmon, L.G., Schauer, J.J., Zeng, L.M., Kiang, C.S., Zhang, Y.H., Cass, G.R., 2005. Seasonal trends in $PM_{2.5}$ source contributions in Beijing, China. Atmos. Environ. 39, 3967–3976.